Proceedings of the 2nd International Conference on Structural Applications of Mechanical Alloying, Vancouver, British Columbia, Canada, 20-22 September, 1993

Strength and Interfacial Structure of Capacitor Discharge Welded Mechanically Alloyed Aluminum

J.A. Hawk, R.D. Wilson, and C.P. Dogan
U.S. Bureau of Mines
Albany, Oregon

Abstract

The Bureau of Mines is studying the influence of capacitor discharge welding (CDW) on alloy microstructures and assessing the effects of welding parameters on fusion and heat affected zone formation. Mechanically alloyed (MA) aluminum affords unique opportunities to study the effect of this low heat input process on nonequilibrium microstructures. In this study, samples of IN-9021 and MA AlTi have been CDW to form similar metal joints. In addition, dissimilar metal welds have been formed by CDW of MA AlTi to commercially pure Ti and Ti-6Al-4V. The strengths of the resulting joints have been determined from tensile tests of the welded samples. Microhardness measurements have also been used to assess the quality of the joint. Optical, scanning and transmission electron microscopy have been used to study the failure characteristics of the weld and changes in the microstructure due to the welding process.

ALLOYS WITH NONEQUILIBRIUM MICROSTRUCTURES hold great promise for the creation of advanced materials having improved mechanical properties. However, these alloys have little commercial utility unless their unique microstructures can be retained during fabrication and joining. In many instances this requires that the thermomechanical cycles associated with part manufacture and joining not exceed the temperature maximum experienced by the material. One possible method of joining these materials is capacitor discharge welding (CDW), a rapid solidification technique (1) that has evolved into an efficient technique for stud welding (2). In CDW, energy is applied for very short times to create a shallow layer of molten metal, which cools very rapidly (10^6 K/s) when in contact with a large thermal heat sink. The resulting fusion zone (FZ) is narrow, and the heat affected zone (HAZ) is virtually nonexistent. Further, the nonequilibrium characteristics of the parent microstructure can be retained, with very few defects, right up to the weld interface.

The CDW process involves gravity assisted, axial impact of cylindrical specimens with subsequent arcing and melting (and thus joining) by the discharge of a capacitor bank. During impact the arc is extinguished, and any excess molten metal is expelled as solidification occurs. Attractive features of CDW include the suppression of FZ porosity due to hydrogen uptake and a minimal HAZ (3). In addition the welds tend not to hot crack because of the compressive forces developed during the welding cycle. Thus the microstructure near the weld is characteristic of the base metal and is affected little by the joining process. The width of the fusion zone can be controlled by varying the welding parameters, which in turn control the cooling rate (4-6). For example, a slow cooling rate (10^5 K/s) leads to a larger FZ. Faster cooling rates (>10^6 K/s) result in much narrower FZs.

Capacitor discharge welding can frequently be used when conventional fusion welding techniques result in poor weld quality. It has been successfully applied to Al-Fe-Ce alloys (7,8) developed for high-temperature applications (9), in which the inherently high hydrogen content of the alloy results in excessive FZ porosity during conventional welding processes. In addition the slow cooling rates associated with conventional welding allow the formation of undesirable, near-equilibrium intermetallic phases with a concomitant coarsening of the Al grains. This results in weld joints that are "soft" because of relatively large fusion and heat affected zones and associated porosity. On the other hand, the microstructure of CDW Al-Fe-Ce joints is quite similar to that of the as-processed, rapidly solidified powder used to make the alloys. The amount of FZ porosity is greatly reduced and localized at the weld centerline, the hardness of the welded region often exceeds that of the base metal, and the overall width of the fusion and heat affected zones is on the order of 80 to 100 μm (7,8). The success of CDW Al-Fe-Ce powder metallurgy alloys has raised the possibility of using this technique to join other non-equilibrium, fine scale

microstructures, such as mechanically alloyed (MA) aluminum.

Materials and Experimental Procedure

The materials used in this study were a MA AlTi alloy and an IN-9021 alloy (hereafter referred to as AlTi and 9021, respectively), both produced by Inco Alloys International, Inc. (IAII). The composition of the AlTi alloy was: Al(bal)-10.0Ti-0.1Fe-0.9O-1.7C (all values in weight percent). The 9021 alloy is similar in chemical composition to AA2024 except for the high oxygen and carbon content and the absence of Mn, and has the nominal composition: Al(bal)-4.0Cu-1.5Mg-0.8O-1.1C (10). Both of these alloys contained oxides and carbides which were assumed to be primarily Al_2O_3 and Al_4C_3, although other complex oxides and carbides might also be expected. Commercial purity Ti and Ti-6Al-4V (Ti-6-4) were used in the dissimilar metal CDW experiments.

A schematic diagram of the CDW process is shown in Figure 1. The heat input is very intense, and extremely brief, usually only lasting between 0.5 and 4 ms. In this study, the drop height, drop weight, temperature and voltage were varied as shown in Table 1, allowing both fast and slow cooling rates within the weld (3,6,8). All tests used an ignition tip length of approximately 1.01 mm and a capacitance of 80,000 μF.

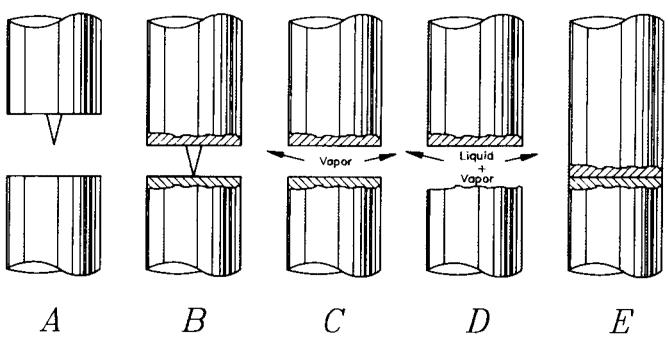

Fig. 1 - Schematic representation of the CDW process. (a) Starting configuration; (b) cathode (tip) approaching anode with spark ignition and heat generation; (c)-(d) formation of vapor and liquid due to high heat generation ; and (e) surfaces contacting with expulsion of vapor and liquid.

Optical microscopy and transmission electron microscopy (TEM) of the FZ and HAZ were performed on selected samples sectioned transverse to the weld centerline. Microhardness measurements (300 g load) were made from the base metal on one side of the weld centerline through the FZ and into the base metal on the other side of the weld centerline. Tensile tests were also performed on CDW samples, as per the welding conditions listed in Table I, using a screw driven tensile test machine. Comparative tensile specimens of AlTi were 76 mm in length, with a gauge length of 30 mm and a gauge diameter of 6.4 mm. A crosshead speed of 0.5 mm/min was used for all tests, giving an effective strain rate of 3.3×10^{-4} /s. Fractographic analyses of all of the tensile tested specimens were performed using scanning electron microscopy (SEM). Samples for TEM analysis were prepared by sectioning thin slices of the material transverse to the weld centerline, electro-discharge machining 3 mm diameter disks and electropolishing in a 1:3 (by volume) solution of nitric acid and methanol at 255 K. TEM analyses were performed at 100 kV.

Results and Discussion

Similar Metal Welds. Weld strengths for similar metal welds are listed in Tables II and III, respectively. Joint efficiencies, defined as the ratio of weld strength to the ultimate tensile strength of the appropriate alloy, are also included in Tables II and III. For AlTi, a tensile strength of 568±3 MPa was determined from the average of 3 tensile tests on cylindrical specimens pulled under conditions identical to those used for the CDW samples. A tensile strength of 538 MPa for the 9021 alloy was taken from the literature (10).

For the AlTi CDWs, weld strengths vary from a low of 279 MPa (joint efficiency of 49%) to a high of 460 MPa (joint efficiency of 81%). With one exception, all samples failed either in the HAZ or along the weld centerline (WCL). Sample AlTi(5) fractured in the base metal near the grips. No attempt has been made to optimize the weld parameters; however, welds made at 90 V produced the least effective welds. The most consistent weld strengths were obtained at 80 V, with drop height and drop weight affecting the strength in only a minor way. In the limited number of samples tested, there appears to be a slight trend towards increased joint efficiency with increasing drop height. According to theory (3-6), if all other welding conditions are constant, increasing the drop height will lead to an increase in the solidification rate by reducing the welding time.

Figure 2(a) shows a transverse cross-section of the HAZ, while 2(b) is the fracture surface of sample AlTi(1). Generally, large voids are absent within the FZ, although some minor cracking in the HAZ is apparent. The actual FZ is, on average, 8 μm in width, and the HAZ is between 50 and 130 μm in width. Microhardness measurements showed that the HAZ and FZ were "softer" than the base metal. The base metal microhardness varied from approximately 165 kg/mm^2 (one side of the weld centerline) to 172 kg/mm^2 (other side of the weld centerline). The microhardness of the HAZ and FZ was 135 kg/mm^2. The reduction in microhardness from base metal to HAZ is approximately 20%. Examination of the fracture surface plane confirms the

Table I. Capacitor Discharge Weld Parameters.

Weld Cond	Diameter (mm)	Capacitance (μF)	Voltage (V)	Drop Height (mm)	Drop Weight (kg)	Tip Length (mm)
A	6.4	80,000	90	38	1.9	1.01
B	6.4	80,000	80	25	1.9	1.01
C	6.4	80,000	80	38	1.9	1.01
D	6.4	80,000	80	51	1.9	1.01
E	6.4	80,000	80	38	0	1.01
F	6.4	80,000	70	38	0	1.01

Table II. MA AlTi Similar Metal Welds.

Specimen Number	Weld Cond	Weld Strength (MPa)	Joint Efficiency (%)	Fracture Location
AlTi(1)	A	361	64	HAZ
AlTi(2)	A	279	49	WCL
AlTi(3)	B	413	73	WCL
AlTi(4)	C	444	78	WCL
AlTi(5)	C	429	76	BM
AlTi(6)	D	460	81	WCL
AlTi(7)	E	380	67	WCL
AlTi(8)	F	455	80	HAZ

BM-base metal outside of interface or heat affected zone
IR-interface region (i.e., region adjacent to heat affected zone)
HAZ-heat affected zone
WCL-weld centerline

Table III. IN-9021 Similar Metal Welds.

Specimen Number	Weld Cond	Weld Strength (MPa)	Joint Efficiency (%)	Fracture Location
9021(1)	A	336	62	WCL
9021(2)	A	100	19	WCL
9021(3)	B	352	65	BM
9021(4)	C	281	52	WCL
9021(5)	D	282	52	WCL

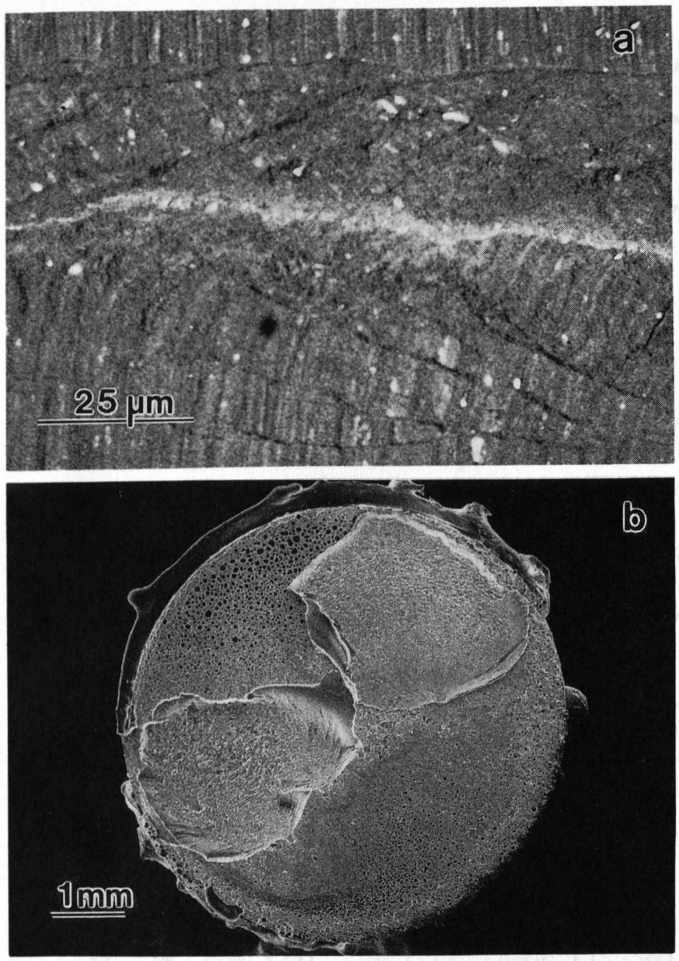

Fig. 2 - (a) SEM micrograph of CDW cross-section and (b) fracture surface at the weld interface for AlTi.

absence of large voids due to the welding process. With an average strength of 403 MPa and an average joint efficiency of 71%, the AlTi gives physically good welds.

The 9021 material, on the other hand, consistently produces weaker joints. Weld strengths range from a lov value of 100 MPa (19% joint efficiency) to a maximum in excess of 352 MPa (65% joint efficiency). The reduction in weld strength is somewhat reflected in the microhardness measurements. The base metal microhardness for 9021 ranged from 166 kg/mm^2 (one side of the weld centerline) to 177 kg/mm^2 (other side of the weld centerline). The microhardness within the HAZ and FZ showed considerable variation (*i.e.* from 123 to 137 kg/mm^2) with an average microhardness of 130 kg/mm^2. From the microhardness measurements, the HAZ is approximately 25% lower in hardness than the adjacent 9021 alloy. Figure 3 shows the transverse cross-section of the weld and the fracture surfaces for 9021. The HAZ of the 9021 alloy is clearly visible, with an overall width of approximately 52 µm. Many small voids are also seen throughout the HAZ. Careful examination reveals an area equivalent to the FZ toward the middle of the HAZ, with an average width of around 13 µm, although this is difficult to measure since the FZ of the 9021 welds is not as clearly visible as that of the AlTi alloy. The plane of the weld interface in these materials frequently contains several large and many small voids (Fig. 3(b)). By using larger compressive forces during the weld cycle (*i.e.* increasing the drop weight), it may be possible to keep in solution any gases that evolve during the CDW process. This would eliminate many of the small voids seen in Figure 3(a).

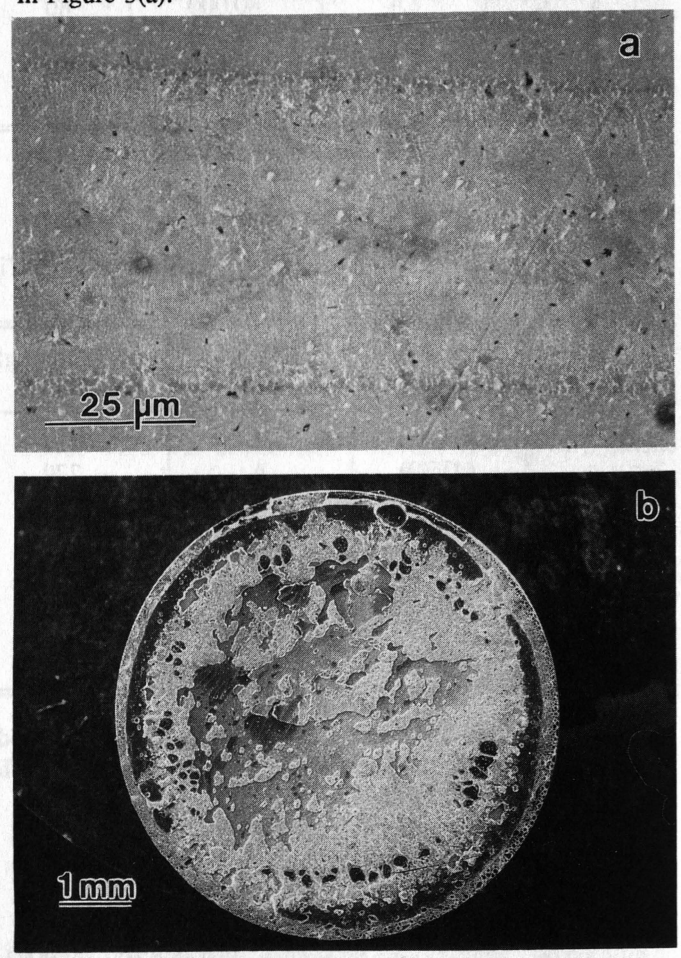

Fig. 3 - (a) SEM micrograph of CDW cross-section and (b) fracture surface at the weld interface for 9021.

Transmission electron microscopy can, however, provide some insight into the question of why the 9021 weld joints are weaker than the AlTi joints. Figure 4 illustrates the microstructure of the AlTi in the bulk regions (Fig. 4(a)), well away from the FZ, and in the region near the FZ (Fig. 4(b)). Away from the weld, the microstructure consists primarily of Al, with a grain size of between 100 and 300 nm, and Al_3Ti, with a size of 20 to 250 nm. In addition there are fine particles of aluminum oxide (Al_2O_3) and aluminum carbide (Al_4C_3) scattered throughout. The Al_2O_3 particles are generally irregular in shape, whereas the Al_4C_3 particles can be described as cylindrical, with a diameter of 20 nm and a

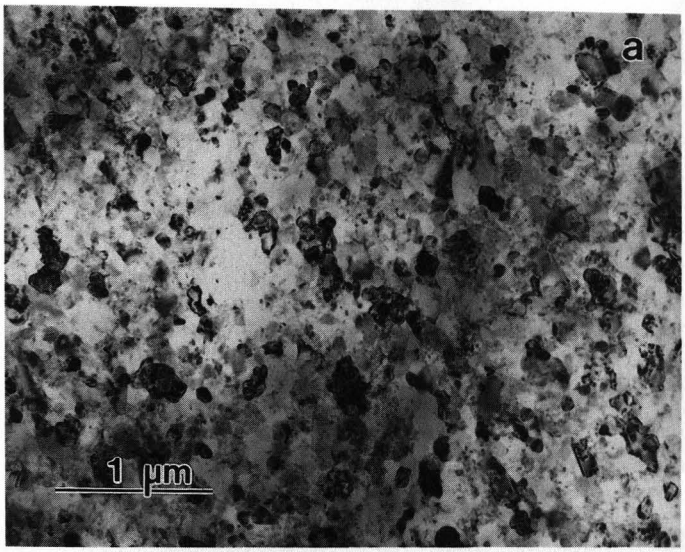

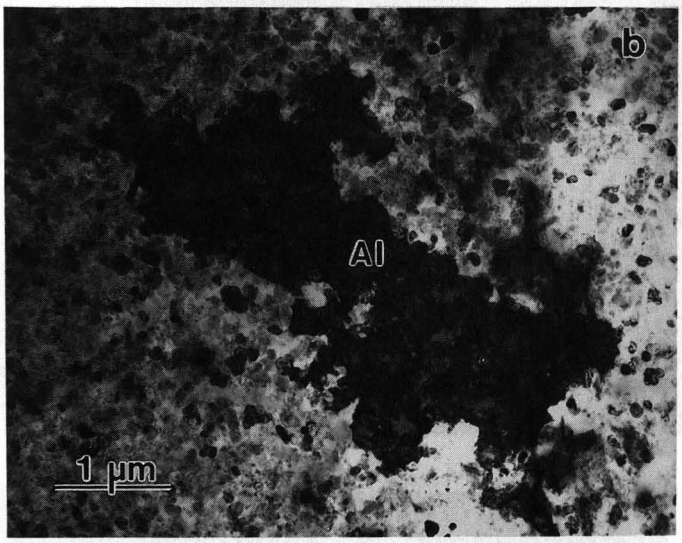

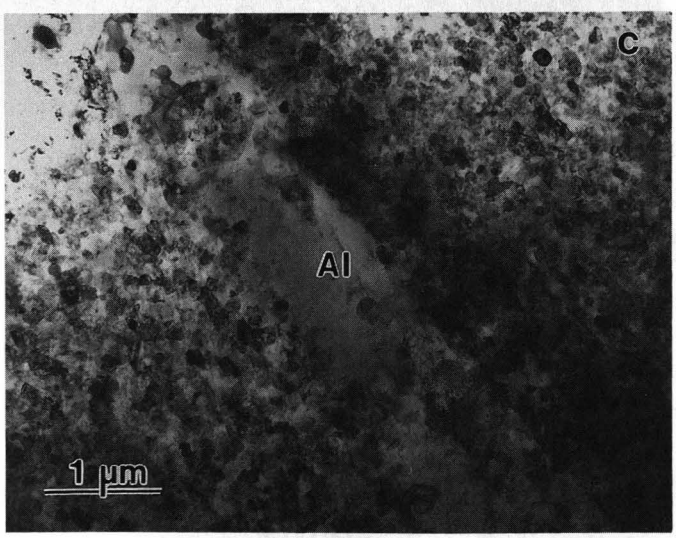

Fig. 4 - AlTi microstructures (TEM): (a) the bulk material away from the HAZ and (b) the region of the HAZ near the FZ. (c) Columnar aluminum grain growth due to the CDW process in the HAZ.

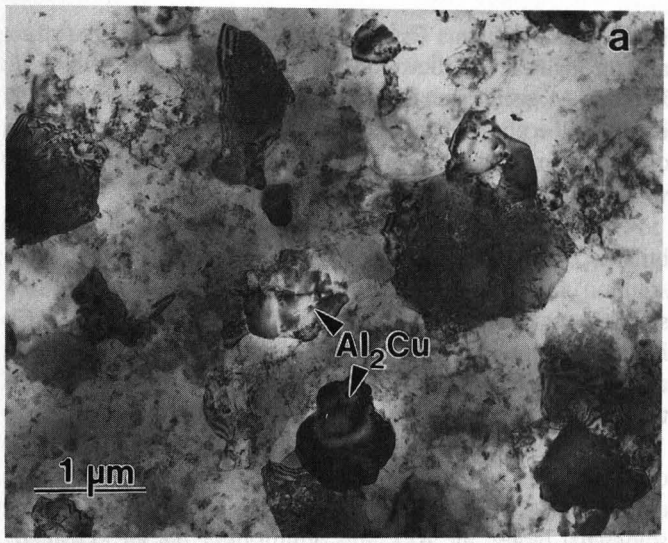

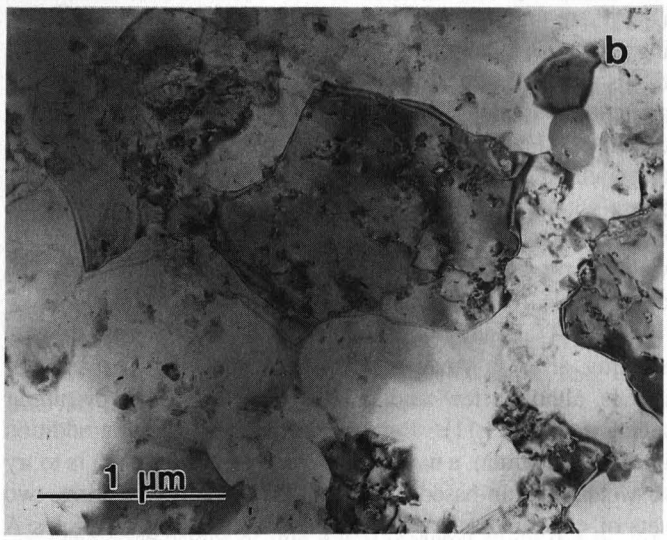

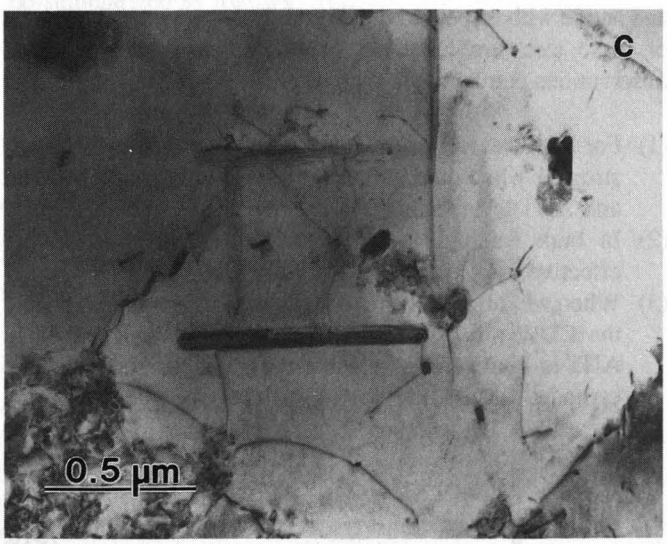

Fig. 5 - 9021 microstructures (TEM): (a) bulk material away from the HAZ and (b) the region of the HAZ. The actual interface and FZ are not apparent. (c) Large intragranular precipitate in the HAZ.

length of 50-200 nm. This microstructure persists right up to, and through the FZ, but with several differences: Within the FZ, the Al grain size is much increased, whereas the Al_3Ti intermetallic phase appears unchanged (Fig. 4(b)). In addition, columnar grains of crystalline Al form perpendicular to the weld interface, as illustrated in Figure 4(c).

Microstructural analyses of CDW 9021 indicate that the bulk is composed primarily of Al grains (with a trace of Cu in solution) that have a high dislocation density and contain rod-shaped intragranular precipitates (Fig. 5(a)). Tetragonal Al_2Cu is the most frequently observed intermetallic phase formed in this alloy; it too contains some intragranular precipitates. A tetragonal Al_7Cu_2Fe and an Al-Mg phase are also present.

The HAZ of the 9021 welded material (Fig. 5(b)) consists of a narrow region of somewhat larger Al grains, however, the actual interface and FZ are not apparent. In addition to being somewhat larger, the Al grains within the HAZ are "cleaner", i.e., there are fewer dislocations and there are fewer intragranular precipitates. The intragranular precipitates themselves are larger, and the rod-shaped ones (Figure 5(c)) are tentatively identified as Al_4Cu. There are also fewer Al_2Cu and Al_7Cu_2Fe grains within the HAZ. The lack of these dispersoids, combined with the absence of a fine precipitate phase within the Al grains, suggests a weaker region near the weld interface. Combined with the voids formed during the welding process, a weaker joint is expected, and is in fact observed.

AlTi-Ti Dissimilar Metal Welds. Capacitor discharge welding offers a novel and efficient way to join dissimilar metals, although few studies have been devoted to dissimilar metal welding (3,11). Because the primary alloying addition in AlTi is titanium, a natural extension of this research is to try to weld titanium-based alloys to AlTi. At this writing, two sets of experiments have been performed, using schedules A and C in Table I, and alternating the AlTi alloy as the cathode and anode with respect to the Ti and Ti-6-4 alloys. The results of these tests are found in Table IV. Several interesting observations can be made from these experiments:

(1) For both welding trials, joints are approximately 50 times stronger when titanium alloys serve as the anode material and AlTi is the cathode.
(2) In both welding trials, a Ti-6-4 anode forms a more effective joint with the AlTi alloy.
(3) When welding Ti-alloys to AlTi, the total mass loss during the CDW process is approximately twice as great when AlTi is the cathode as when the Ti-alloys serves as the cathode. More mass is lost from the titanium alloy regardless of whether it serves as the anode or the cathode.

Figure 6 shows transverse cross-sections of the AlTi-titanium based dissimilar metal welds. Generally, when AlTi is the cathode (Fig. 6(a)), the HAZ appears to be relatively free of voids and cracks, with relatively large intermetallic phases present. When the titanium alloys are used as the cathode, intermetallic phase formation still occurs but cracking in the HAZ is more prevalent (Fig. 6(b)). A number of small voids are seen in the Al-rich side of the HAZ, and there is some cracking in the HAZ near the intermetallic phases.

Measurement of HAZ width in the dissimilar metal welds is difficult; however, the following has been observed: For the AlTi-Ti couples, the HAZ width when AlTi is the cathode is approximately 44 μm, while the width of this zone when Ti is the cathode is 54 μm. For the CDW AlTi-(Ti-6-4) couples, the HAZ width when AlTi is the cathode is 55 μm, while this width is only 26 μm when Ti-6-4 is the cathode.

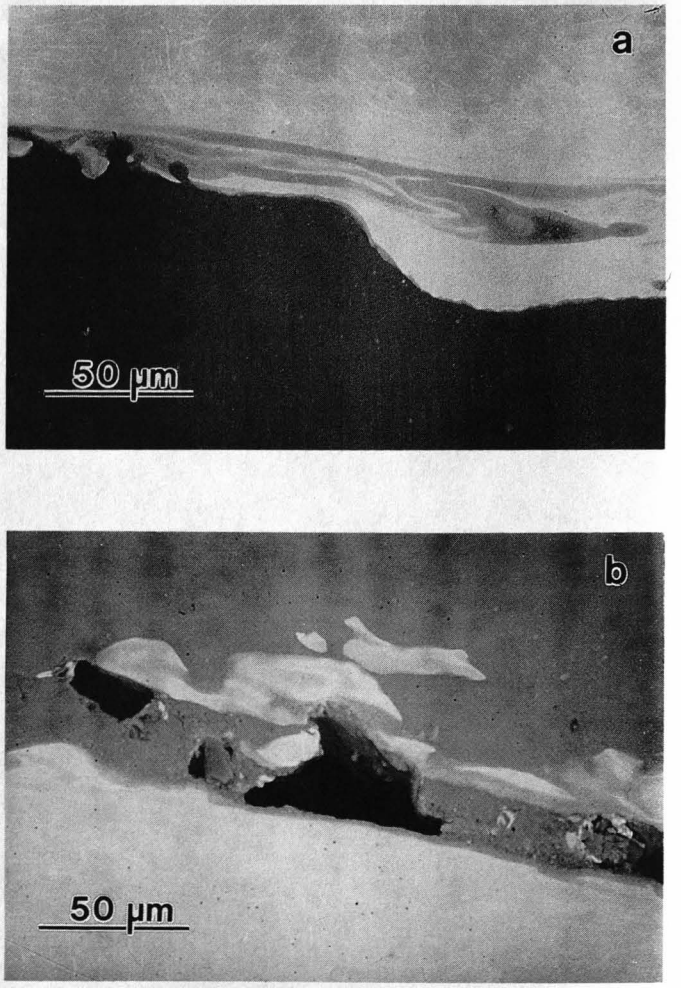

Fig. 6 - SEM micrographs of transverse cross-sections of the AlTi-Ti based alloy dissimilar metal welds. (a) Case where AlTi is the cathode (i.e., "good" weld) and (b) the case where Ti is the cathode (i.e., "poor" weld).

The startling difference in joint quality with cathode material is equally apparent when looking at the fracture

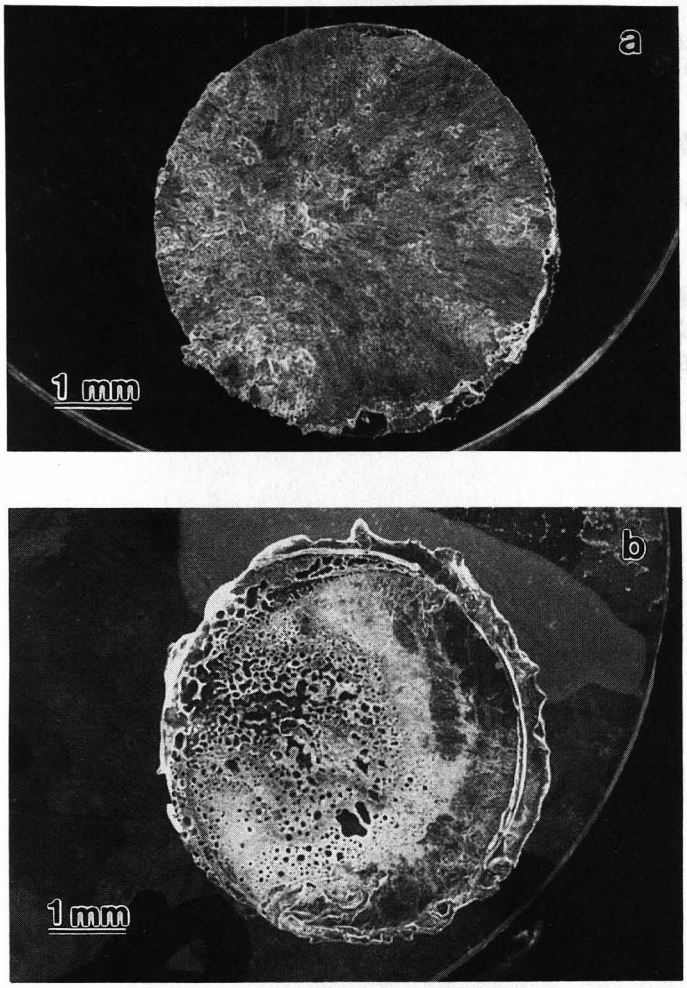

Fig. 7 - SEM micrographs of fracture surfaces of the AlTi-Ti dissimilar metal welds. (a) Fracture surface when AlTi is the cathode. (b) Fracture surface of joint when Ti-6-4 is the cathode. Note the large voids, an indication of poor adherence during CDW.

surfaces of the dissimilar AlTi-(Ti-6-4) metal welds. Figure 7(a) is the fracture surface of the weld when AlTi is the cathode. The plane of the surface does not contain any voids, and failure occurs along the WCL in a uniformly ductile manner. The overall quality of the weld is good. When Ti-6-4 is the cathode, Figure 7(b), the fracture surface contains many large voids and has areas where bonding does not occur. It is clearly evident that the strength of the joint is poor. In doing microhardness profiles across the WCL from the aluminum side to the titanium side, it appears that the choice of cathode material also makes a significant difference in the microhardness of the weld. For example, the microhardness of the HAZ for AlTi-(Ti-6-4) couples is higher when Ti-6-4 is used as the cathode (235 kg/mm^2), compared to the case when AlTi is used as the cathode (162 kg/mm^2). The average microhardness of the AlTi does not change when it is used as the anode or the cathode (*i.e.* it remains on average 155 kg/mm^2). The microhardness of the AlTi is considerably less after CDW with Ti-6-4 (155 kg/mm^2 compared to approximately 170 kg/mm^2 when AlTi is welded to itself). The same general trend holds for the AlTi-Ti CDW couples. From microhardness measurements alone, it would appear that AlTi-titanium alloy welds are stronger when a titanium alloy is the cathode. This would seem to contradict the tensile data were it not for the fact that more cracking occurs when the titanium alloys are used as the cathode. More study is needed to clarify the results of these experiments. TEM analysis will aid in the explanation, but preparing specimens with sufficient thin area for TEM analysis has proven difficult.

Conclusions

The conclusions of this initial research study can be can be summarized as follows:

Table IV. AlTi-Titanium Dissimilar Metal Welds.

Weld Cond	Cathode	Anode	Total Mass Loss (g)	Joint Strength (MPa)
A	AlTi	Ti	-----	228.0
	AlTi	Ti-6-4	-----	318.0
	Ti	AlTi	-----	6.6
	Ti-6-4	AlTi	-----	4.9
C	AlTi	Ti	0.0373	113.0
	AlTi	Ti-6-4	0.0310	201.0
	Ti	AlTi	0.0157	----
	Ti-6-4	AlTi	0.0161	----

(i) CDW can be an effective method of joining complex aluminum alloys with nonequilibrium microstructures. Joint integrity is generally good with a narrow HAZ (~80 μm). There is no softening of the material at the joint due to microstructural changes. In most cases, the joint efficiency of AlTi similar metal welds is greater than 70%.

(ii) Welding dissimilar metals is possible but the physical properties of the alloys being welded will determine which material should be used as the anode and which material will be more effective as the cathode.

Preliminary results suggest that the lower melting temperature material should be the cathode. However, further research is needed to optimize the welding parameters for MA aluminum base alloys and dissimilar metal couples.

Acknowledgments

The authors would like to express their appreciation to J. H. Devletian for the use of the CDW apparatus; to A. Watwe (IAII) for supplying the MA AlTi alloy; to N. Duttlinger for specimen preparation and optical microscopy; and to K. Collins for performing the scanning electron microscopy.

References

1 Jones, H., Mater. Sci. Eng., 5, 1-18 (1969).
2 Shoup, T. E., C. C. Pease and M. Tamiuasu, "Metals Handbook, 9th Ed., Vol. 6," p. 729, ASM, Metals Park, OH (1983).
3 Devletian, J. H., Weld. J., 66, 33-39 (1987).
4 Venkataraman, S. and J. H. Devletian, Weld. J. (suppl.), 67, 111s-118s (1988).
5 Venkataraman, S. and J. H. Devletian, "Principles of Solidification and Materials Processing, Vol 2," p. 859, Trans Tech, New York (1988).
6 Einerson, C. J., D. E. Clark and J. H. Devletian, "ASME/JSME Thermal Engineering Joint Conf., Vol 3," p. 217, ASME, New York (1987).
7 Baeslack, W. A., K. H. Hou and J. H. Devletian, J. Mater. Sci. Lett., 7, 944-948 (1988).
8 Baeslack, W. A., K. H. Hou and J. H. Devletian, J. Mater. Sci. Lett., 8, 716-720 (1989).
9 Langenbeck, S. L., W. M. Griffith, G. J. Hildeman and J. W. Simon, "Rapidly Solidified Powder Aluminum Alloys," p. 410, ASTM, Philadelphia, PA (1986).
10 Hildeman, G. J. and M. J. Koczak, "Aluminum Alloys-Contemporary Research and Applications," p. 338, Academic Press, San Diego, CA (1989).
11 Wilson, R. D. and J. A. Hawk, (U. S. Bureau of Mines, 1450 Queen Ave. SW, Albany, OR 97321), unpublished research (1992).

Mechanical Alloying for Structural Applications

Proceedings of the
2nd International Conference on Structural Applications of Mechanical Alloying
20-22 September 1993
Vancouver, British Columbia, Canada

Edited by
J.J. deBarbadillo, F.H. Froes, and R. Schwarz

Sponsored by
ASM International®

Production Project Manager
Suzanne E. Hampson

Project Coordinator
Donna-Sue Plickert

Published by
ASM International®
Materials Park, Ohio 44073-0002

First printing, September 1993

This book is a collective effort involving hundreds of technical specialists. It brings together a wealth of information from worldwide sources to help scientists, engineers, and technicians solve current and long-range problems.

Comments, criticisms, and suggestions are invited, and should be forwarded to ASM International.

Library of Congress Cataloging Card Number: 93-79328
ISBN: 0-87170-492-7
SAN: 204-7586

ASM International®
Materials Park, OH 44073-0002

Printed in the United States of America